Appl. Phys. B 81, 83–91 (2005)
DOI: 10.1007/s00340-005-1860-z

Applied Physics B
Lasers and Optics

N.N. IL'ICHEV[1]
A.V. KIR'YANOV[1,2,✉]
V.P. SHAPKIN[3]
S.A. NASIBOV[3]
S.YE. MOSALEVA[1]

Nonlinear change in refractive index of Co^{2+}:ZnSe at short-pulse single-beam 1.54-μm *Z*-scan probing

[1]A.M. Prokhorov General Physics Institute, Russian Academy of Sciences, Vavilov Str., 38, 119991 Moscow, Russian Federation
[2]Centro de Investigaciones en Optica A.C., Loma del Bosque #115, Col. Lomas del Campestre, 37150 Leon, Guanajuato, Mexico
[3]P.N. Lebedev Physical Institute, Russian Academy of Sciences, Leninskii Pr., 53, 119991 Moscow, Russian Federation

Received: 7 January 2005 / Revised version: 15 March 2005
Published online: 3 June 2005 •

ABSTRACT An experimental study and theoretical modeling of the nonlinear change in refractive index of a Co^{2+}: ZnSe crystal at the short-pulse single-beam probing at the wavelength 1.54 μm is reported. In the experimental conditions of negligible contributions in the index non-linearity stemming from the Kerr-effect and inhomogeneous heating, the nonlinear change in refractive index in Co^{2+}:ZnSe is shown to be caused by the resonant Co^{2+} population-perturbation effect (i.e., by the Co^{2+} ground-state absorption saturation). The *Z*-scan single-beam technique and novel theoretical approach addressing the resonant nonlinear refraction in a saturable doped medium are used, respectively, for an experimental and theoretical inspection of the phenomenon. For a set of Co^{2+}:ZnSe samples with different concentrations of Co^{2+} ions at the short-pulse (200 ns) mJ-range probing, we show that the maximal nonlinear change in refractive index is about of units of 10^{-4} at the chosen wavelength.

PACS 42.70.Hj; 42.65.Hw; 42.60.Gd; 78.20.Nv

1 Introduction

During the last few years, Co^{2+}:ZnSe crystal became a popular material for the use as a passive Q-switch component in Erbium bulk and fiber lasers (wavelength $\lambda =$ 1.54 μm) allowing their reliable giant-pulse operation [1–5]; Co^{2+}: ZnSe crystal is also a promising active medium for lasing in the mid-IR (3–3.7-μm) spectral range [6]. Despite Co^{2+}: ZnSe is a relatively novel laser crystal, to the date only a few studies have been performed with this material, with a part of them relating to the investigation of the nonlinear (intensity-dependent) transmission of the crystal [7–11] for determining such an important parameter as cross-section of the $^4A_2(^4F)$–$^4T_1(^4F)$ transition responsible for the bleached (saturated) absorption at the wavelengths λ =1.4–1.9 μm. Note that this parameter stays uncertain—the estimates for the resonant (ground-state) absorption (GSA) cross-section at λ =1.54 μm span from 7.6×10^{-19} to 11.5×10^{-19} cm^2. An important point of interest is the residual absorption in Co^{2+}:ZnSe: There are two possible explanations for this feature—the excited-state absorption (ESA) from the $^4T_1(^4F)$ level and linear losses due to the absorption on other impurities (rather than Co^{2+} ions) formed at the crystal's growing and doping. It is difficult to separate these sources of residual absorption in a doped crystal [12, 13] since both the phenomena are modeled by the same law, the Avizonis–Grotbeck equation [14]. However, the second explanation seems to be a more realistic since there are no properly lying resonant levels where the Co^{2+} ions may transit from the $^4T_1(^4F)$ state at the wavelength 1.54 μm. In addition, an experimental confirmation was reported for this hypothesis based on the investigation of a set of Co^{2+}:ZnSe crystals, including the ones totally free from the residual losses [11]. That is why in our modeling (see below) we take as the most relevant the value of the GSA cross-section in Co^{2+} :ZnSe as $\sigma_{GSA} = 11 \times 10^{-19}$ cm^2 (λ =1.54 μm) and neglect the ESA transition ($\sigma_{ESA} = 0$), implying existence of only passive (non-resonant) losses in the crystal. Let us stress that Co^{2+}:ZnSe samples treated in the course of our experiments were the same as in [11].

Note that in spite of significant interest to the Co^{2+}:ZnSe crystal, there is a lack of data in the literature on nonlinear refraction in this material at the wavelength $\lambda = 1.54$ μm, in particular, on the refractive index change Δn^{res} caused by the GSA saturation under powerful excitation. This change in the refractive index appears as the necessary counterpart for the resonant-absorption effect and can be addressed theoretically in the frames of the known Kramers–Kronig Relations, KKR [15, 16]. To the best of our knowledge, only in a single work [17] are inspected some features of nonlinear refraction in Cr^{2+}-doped II–VI laser materials (note here that the properties of the Cr^{2+}-doped materials are somewhat similar to those of the Co^{2+}-doped ones).

✉ Fax: +7(095)135-2055, E-mail: kiryanov@cio.mx

In the following sections, we investigate, both experimentally and theoretically, the resonant contribution Δn^{res}in the refractive index change in Co^{2+}: ZnSe. Other possible sources for the index change may be totally omitted in our experimental conditions where short-pulse probing is used (see below). This holds as for the part Δn^{TL}, the change associated with the thermo-lensing effect in a doped crystal owing to inhomogeneous heating (which is significant at CW or quasy-CW excitation only [18]), as for the part $\Delta\, n^{\mathrm{K}}$, the change stemming from the Kerr-effect, which is pronounceable at a much less duration of an incident pulse [19].

Therefore, the resonant nonlinear change in the index ($\Delta\, n^{\mathrm{res}}$) of Co^{2+}: ZnSe, which corresponds to saturation of the GSA $^4A_2(^4F) - {}^4T_1(^4F)$ transition, is of the present report's scope. This effect is inspected by us applying the well-known Z-scan technique [20]. We also introduce a new theoretical model for the resonant (nonlinear) refraction in a doped crystal at short-pulse excitation and apply the results of this modeling to the case of a Co^{2+}: ZnSe doped crystal.

2 Experimental setup

An experimental setup for studying the nonlinear change in refractive index Δn^{res} of Co^{2+}: ZnSe by the Z-scan technique is shown in Fig. 1. The samples were (100)-cut Co^{2+}: ZnSe thin plates with different contains of Co^{2+} doping ions (see Table 1); one of the tested samples was a pure ZnSe crystal totally free from Co^{2+}. All the Co^{2+}-doped samples have been prepared applying the method of diffusion at the equilibrium condition, S_{ZnSe}-S_{CoSe}-L_{Zn}-V. This formula implies that the diffusion process goes in the conditions of equilibrium of the solid phase of ZnSe, the solid phase of CoSe, the liquid phase of Zn, and vapors of all the presented phases. This novel technology differs from the traditional ones, the modified diffusion [21] and Bridgman's [22] methods, and allows one to produce highly homogeneous Co^{2+}: ZnSe samples with a high resistance to optical damage (optical breakdown at the wavelength 1.54 μm is observed at energy densities exceeding 10 J/cm^2) [11]. The final samples have been polished and AR-coated for $\lambda = 1.54$ μm (note that refractive index of a "pure" ZnSe crystal is $n = 2.45$). In the course of experiments an incident laser beam was directed almost normally to the samples' facets.

The incidence probe radiation was launched from a bulk Erbium-doped-glass laser (L) ($\lambda = 1.54$ μm) operating at active Q-switching of the cavity with an electro-optical shutter

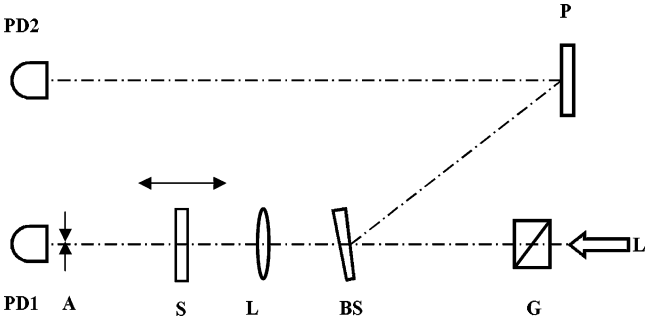

FIGURE 1 Experimental setup

#	T_{in} (%)	T_{fin} (%)	L, (cm)	α (cm)$^{-1}$	γ, (cm)$^{-1}$
343	29.5	74.0	0.083	10.796	3.709
355	39.0	89.0	0.093	8.872	1.253
357	81.0	97.5	0.051	3.605	0.609

TABLE 1 Co^{2+}: ZnSe samples' parameters

on $LiNbO_3$. The duration of giant pulses emitted by the laser was normally around 200 ns; pulses were sequenced at the repetition rate of 0.25 Hz. Maximal pulse energy at the entrance of Co^{2+}: ZnSe samples was about 5 mJ. The distribution of the laser beam was a pure TEM_{00}-mode. The laser beam had a linear (1:1000) state of polarization. A Glan prism (G) set behind the Erbium laser allowed us to vary input energy of pulses on a tested sample (S). A lens (L) with the focal distance of 30 cm was used for focusing probe radiation onto the sample; the beam waist at the focus was $\omega_0 = 114$ μm. Open and closed-aperture Z-scans, characterizing nonlinear transmission and refraction of Co^{2+}: ZnSe (see below), were obtained by splitting the beam with a beam-splitter (BS) and plate (P) and simultaneous registering of the two resultant beams by a pair of similar Germanium Photo-Detectors (PD1 and PD2). For measuring the closed-aperture Z-scans, an aperture (A) of the diameter $\emptyset = 0.514$ mm was set in front of the photo-detector PD1. The two photo-detectors were capable of recording either intensity of a pulse in a fast regime (using the detectors of the LED-2a type with the response rising time less than 1 ns), or pulse energy (in this case, were used the detectors of the FD-7g type equipped with electrical integrating chains in their registering parts). In the first circumstance, the measurements were single-pulse, whilst in the second one each experimental point was obtained after averaging over five shots of the probe laser that provided accuracy of measurements at the level better than 0.5%. Before the main experiments, signals from the photo-detectors were calibrated with the help of a calorimeter placed in the scheme instead of a Co^{2+}: ZnSe sample. The integrated signals from the photo-detectors were recorded with a controller arranged in the KAMAK standard and equipped with a personal computer. At registering intensity of a pulse, we used an oscilloscope (Tektronix TDS744A), which gives temporal resolution of about 2 ns.

The nonlinear (intensity-dependent) changes in a sample's transmission and refractive index Δn^{res} were determined by measuring so-called open-and closed-aperture Z-scans $T0(Z)$ and $T1(Z)$ [20] (Z is the longitudinal coordinate of a Co^{2+}: ZnSe sample with respect to the beam waist). Note that the laser beam was directed along one of the main crystallographic axes of Co^{2+}: ZnSe [001]. A signal from the photo-detector PD1 without an aperture gave us, after division on input power measured by the photo-detector PD2, the open-aperture Z-scan transmission, $T0(Z)$. The closed-aperture Z-scan $T1(Z)$ was obtained by a similar procedure but with the aperture A being placed before the photo-detector PD1 and division of the measured transmission by the transmission $T0(Z)$. In the case of a medium with nonlinear (saturable) absorption, the scans $T0(Z)$ contain the information about the sample's bleaching (due to the GSA saturation), while the scans $T1(Z)$ allow one to determine the nonlinear change in refractive index of the sample. The latter is possible because the aperture A plays

the role of a spatial analyzer of the beam divergence diagram which is influenced by a nonlinear lens induced in the sample.

In the present work, we concentrate our attention on an experimental study of the nonlinear change in refractive index Δn^{res} of the Co^{2+}: ZnSe samples with different concentrations of Co^{2+} ions as well as its dependence on the GSA saturation level (i.e., on the incident energy E_p at the given focusing arrangement). Experimentally, these dependences were measured by recording $T0(Z)$ and $T1(Z)$ Z-scans obtained by moving the sample relatively to the beam waist position, Z_0.

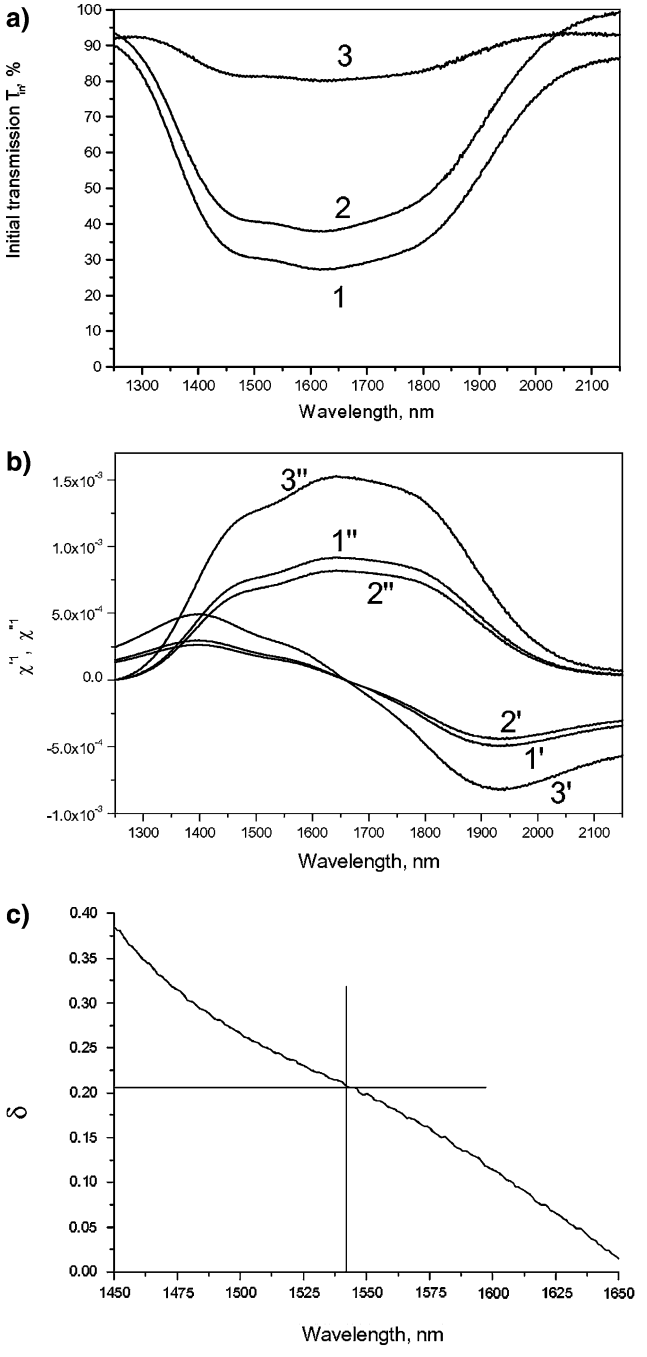

FIGURE 2 Spectra of initial transmission T_{in} **a** and also real (χ'^1) and imaginary (χ''^1) parts of susceptibilities of non-excited Co^{2+}: ZnSe samples. **b** Curves 1, 2, and 3 relate, respectively, to samples #343, #355, and #357. Inset **c** shows how the parameter δ is determined

3 Experimental results

Figure 2a shows the absorption spectra of three Co^{2+}: ZnSe samples (#343, #355, and #357) with the different concentrations of Co^{2+} ions and the related parameters listed in Table 1. These spectra demonstrate all the features of the $^4A_2(^4F) - {}^4T_1(^4F)$ GSA transition, being characteristic for Co^{2+}: ZnSe crystals grown applying other technologies.

An example of the experimental Z-dependent transmission without apertXSure (a), its normalized (on maximum) value (i.e., the open-aperture Z-scan, $T0(Z)$) (b), and normalized ratio of transmissions measured with and without aperture behind the crystal (i.e., the closed-aperture Z-scan, $T1(Z)$) (c) are shown in Fig. 3 for Co^{2+}: ZnSe samples #343 (curves 1), #355 (curves 2), and #357 (curves 3). For comparison, in Fig. 3 are also given the correspondent dependences for the un-doped ZnSe sample labeled as "pure" (curves 0). On these figures, all the plots (a-c) have been obtained for the same energy of the laser pulse, $E_p = 2.3$ mJ. The graphs (a, b) demonstrate the GSA saturation effect under the

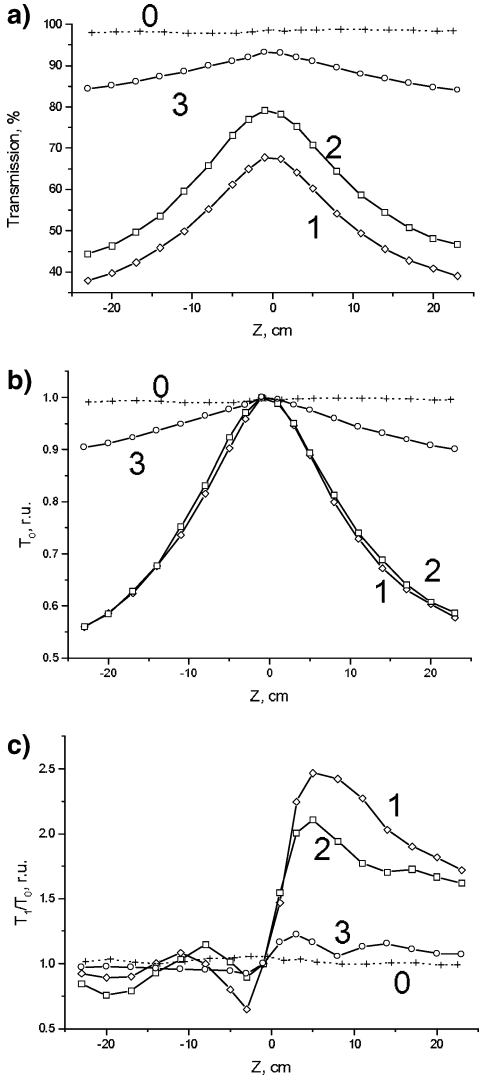

FIGURE 3 Experimental transmission **a** and Z-scans $T0(Z)$ **b** and $T1(Z)$ **c** measured for Co^{2+}: ZnSe samples #343 (*curves 1*), #355 (*curves 2*), #357 (*curves 3*), and "pure" ZnSe sample (*curves 0*). All the experimental data correspond to incidence pulse energy $E_p = 2.3$ mJ

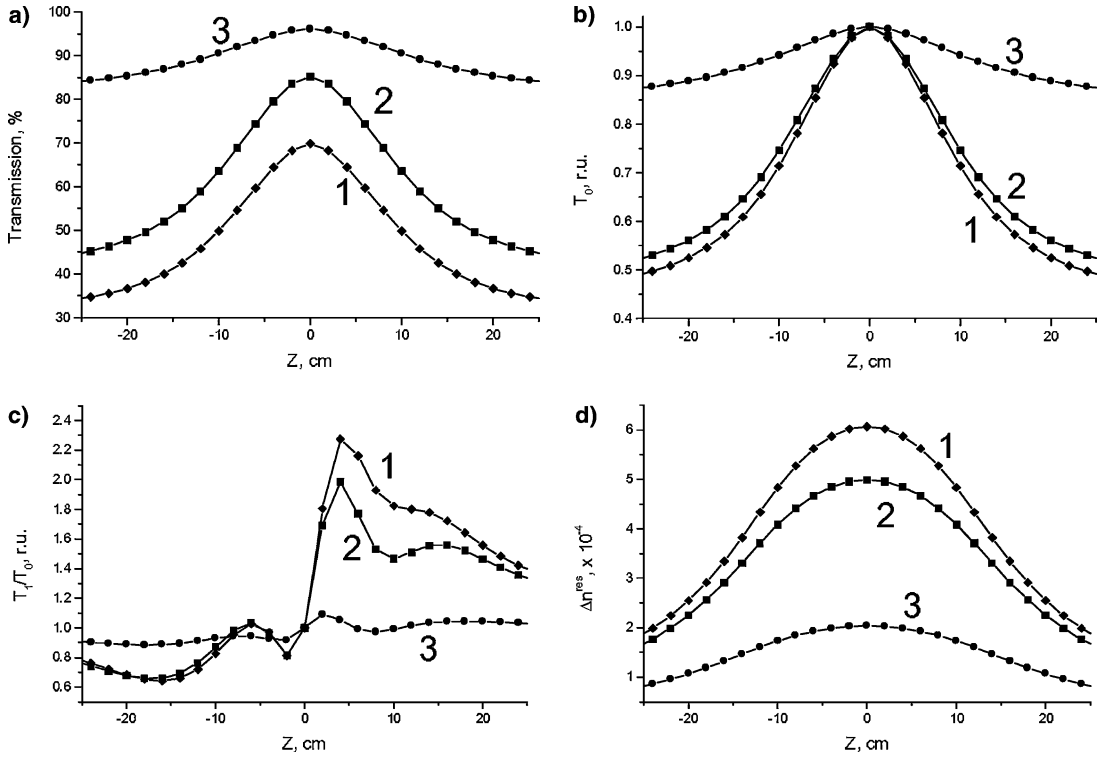

FIGURE 4 Theoretical transmission **a**, Z-scans T0(Z) **b** and T1(Z) **c**, and refractive index change Δn^{res} **d** calculated for Co^{2+}: ZnSe samples #343 (*curves 1*), #355 (*curves 2*), and #357 (*curves 3*). All the data were calculated for incidence pulse energy $E_p = 2.3$ mJ

action of powerful giant-pulse excitation at $\lambda = 1.54$ μm. Note here that samples #343 and #355 which have quite different values of the initial (unbleached) and final (fully bleached) transmissions, T_{in}, and T_{fin}, (see curves 1 and 2 in Fig. 3a), possess of virtually the same resonant (saturable) absorption (see the almost matching $T0(Z)Z$-scans 1 and 2 in Fig. 3b) and, therefore, of quite different residual losses (see Table 1). By the same time, the closed-aperture $T1(Z)$ Z-scans plotted in Fig. 3c which were obtained for the first time to our knowledge for Co^{2+}: ZnSe, demonstrate the nonlinear change in refractive index, the process accompanying the GSA saturation and addressed theoretically (see below) as the change in real part of resonant susceptibility of the crystal. On the other hand, a comparison of the graphs for the Co^{2+}-doped samples (curves 1–3) with the graphs for the un-doped ZnSe sample which all are non-variable with a change of the Z-position (see curves 0 in Fig. 3) testifies additionally for the conclusion that the changes in refractive index of the doped Co^{2+}: ZnSe samples are indeed connected with their bleaching, not with the Kerr non-linearity. (The theoretical Z-scan curves shown in Fig. 4, which are the counter-parts for the experimental curves shown in Fig. 3, are discussed below, see Sect. 4).

In Fig. 5a are shown the closed-aperture Z-scans (obtained by the same way as the ones in Fig. 3c) for sample #355 at different excitation levels, i.e., under the action of giant-pulses with energies $E_p = 1.4$, 2.3, and 4.6 mJ. For other samples (#343 and #357), Z-scans are similar and therefore are out of scope here. The remarkable observation stemming from Fig. 5a is that an increase of input pulse energy leads to a decrease of the peak-to-valley oscillation near the $Z_0 = 0$ point in the $T1(Z)Z$-scans, indicating a deep saturating of

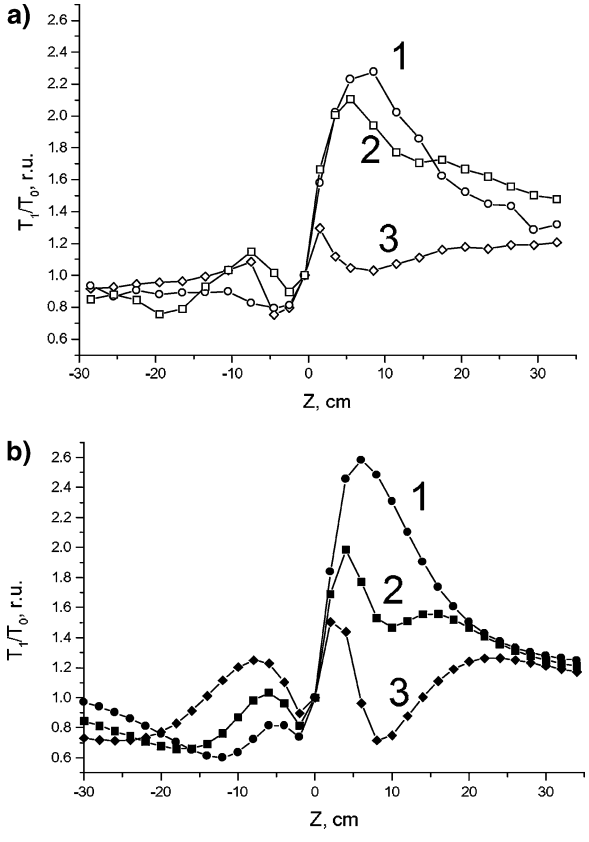

FIGURE 5 Experimental **a** and theoretical **b** T1(Z)Z-scans obtained for Co^{2+}: ZnSe sample #355 at different pulse energy: $E_p = 1.4$ (*curves 1*), 2.3 (*curves 2*) and 4.6 (*curves 3*) mJ

the changes in both the real and imaginary parts of resonant susceptibility and leads, consequently, to deformations of the closed-aperture Z-scans known from the literature [23]. This feature and also a comparison of the experimental dependences (Fig. 5a) with the correspondent theoretical ones (Fig. 5b) will be discussed in more details in Sect. 4.

Note that the presented data have been obtained on the setup where the registering photo-detectors were equipped with integrating chains; that's why all the experimental data in Figs. 3 and 5 are the "integrated" transmissions over the 200-ns pulse-length. Meanwhile, it was interesting to inspect the correspondent instantaneous behaviors of the transmissions $T0(Z)$ and $T1(Z)$. Such temporal dependences are shown in Fig. 6 (again, for sample #355 and fixed pulse energy, $E_p = 2$ mJ), where the photo-detectors were employed without integrating chains in their receiving electrical part (providing "fast" recording of the signals with resolution of 2 ns; these signals were obtained with the Tektronix oscilloscope and processed on the computer). In Fig. 6(a and b) are shown the snapshots of the open-aperture non-normalized ($T0$) and closed-aperture ($T1$) transmissions recorded at the two symmetrical positions of the Co^{2+}: ZnSe sample relatively to the beam waist, $Z = -3.5$ cm (curves 1) and $Z = +3.5$ cm (curves 2). The incidence pulses (on the sample entrance) are plotted in Fig. 6c). It is seen that as the normal transmission of the crystal (Fig. 6a) as the closed-aperture one (Fig. 6b) are the "integrals" over the correspondent incident pulse (Fig. 6c), testifying for that both the effects (nonlinear transmission and nonlinear photo-refraction) to have the same origin –a "slow" saturation of the GSA transition. Notice that the magnitudes of both the effects measured in the last experiment and those obtained in the previous arrangement (where the photo-detectors were equipped with integrating chains) match perfectly.

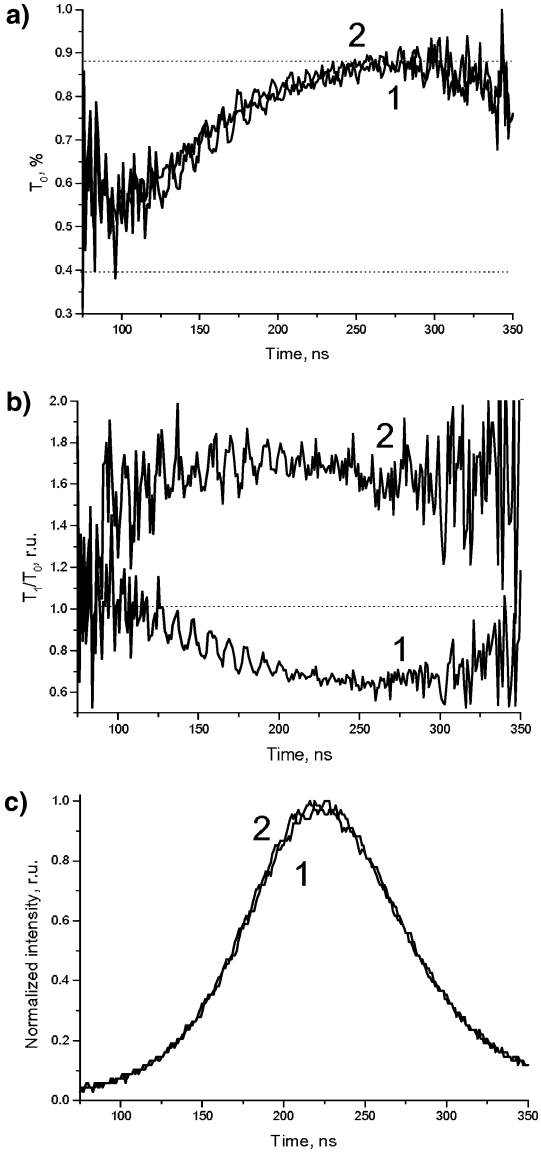

FIGURE 6 Temporal snapshots of transmission **a** and $T1(Z)$ **b** Z-scans measured for Co^{2+}: ZnSe sample #355 at E_p =2.2 mJ. Curves 1 and 2 relate, respectively, to the symmetrical positions of sample with respect to beam waist, −3.5 and +3.5 cm. Figure **c** shows incidence pulse shape for these two measurements

4 Modeling

4.1 *The generalized Avizonis–Grotbeck's equations*

It is known from literature that propagation of a short pulse through a resonantly absorbing (or amplifying) medium with a "slow" relaxation of the excited state is addressed by Avizonis–Grotbeck's equation [14]:

$$\frac{d\varepsilon}{dz'} = -\alpha(1 - e^{-\varepsilon}) - \gamma\varepsilon, \tag{1}$$

where ε is the ratio of the energy density of the incident pulse E_p/s(s is the beam geometrical cross-section) and saturating energy density $E_s = h\nu / \sigma_{GSA}$ ($h\nu$ is the energy quanta at the resonant wavelength), α is the weak-signal resonant absorption coefficient; γ is the residual (non-saturable) loss coefficient, and z' is the current coordinate inside the sample (it should not be confused with the coordinate Z giving the position of a sample with respect to the beam focal point in the Z-scan experiments). Note that Eq. (1) holds in both the cases where the coefficient γ addresses either the passive loss caused by non-resonant impurities (rather than the resonant GSA given by the α coefficient), or the loss relating to a possible presence of the ESA transition at the resonant wavelength. Solving Eq. (1), one is able to calculate the energy-dependent transmission of the medium as the ratio of input (ε_{in}) and output (ε_{out}) energy densities. Therefore, Eq. (1) is sufficient to obtain the theoretical open-aperture Z-scans $T0(Z)$ for Co^{2+}: ZnSe at the wavelength $\lambda = 1.54$ μm at short-pulse probing, implying that the relaxation time of Co^{2+} ions (290 μs [5]) is much bigger than the pulse-width (in our case, about 200 ns).

In order to address the resonant change in the refractive index Δn^{res} in a saturable medium and therefore to calculate the closed-aperture Z-scans $T1(Z)$, one needs to introduce another equation for the phase of the probe radiation (apparently, Eq. (1) characterizes the resonant field amplitude of the pulse). To do so, one should start from Maxwell's equation for the complex field amplitude E^0 of radiation interacting with a single GSA transition, which connects the two resonant states, 1 (lower) and 2 (upper).

At the approximations (i) of slowly changing variables and (ii) of a thin sample (which is a demand of that the time derivative be omitted as a short-pulse propagates through the sample, $\frac{n}{c}\frac{\partial E^0}{\partial t} \langle\langle \frac{\partial E^0}{\partial z}\rangle\rangle$, and (iii) in the conditions that pulse-width is much shorter than relaxation time of the upper level, one can get the following equation:

$$\frac{\partial E^0}{\partial z'} + \frac{E^0\gamma}{2} + \frac{\alpha E_0}{2}\left[\frac{N^1}{N_0} - i\frac{(\chi'^1 N^1 + \chi'^2 N^2)}{\chi''^1 N_0}\right] = 0, \quad (2)$$

where $N^{1,2}$ are the populations of dope centers in the ground and excited state, respectively (where $N_0 = N^1 + N^2$) and $\chi^{1,2} = \chi'^{1,2} + i\chi''^{1,2}$ are the complex susceptibilities in the ground and excited state (with $\chi'^{1,2}$ and $\chi''^{1,2}$ being their real and imaginary parts). Therefore, the following assumptions are additionally implied at the derivation of Eq. (2): (i) Populations of only two states are involved in the changes of the amplitude and phase of the propagating pulse and (ii) susceptibility χ introduced above is meant to be a sum of susceptibilities in these two states. Such a simple equation holds if the ESA and gain g are neglected at the chosen wavelength (i.e., $\sigma_{\mathrm{ESA}} \to 0$; $\chi''^2 \to 0$). Notice that the introduced above low-signal absorption coefficient α relates to imaginary part of susceptibility χ''^1 as $\alpha = \frac{4\pi\omega^2}{c^2}\chi''^1 N_0$.

Assuming that only two levels (1 and 2) are involved in the changes of the amplitude and phase of the propagating pulse and that the complex amplitude E^0 is written as $E^0 = Ee^{i\varphi}$(with E and φ being the electrical amplitude and optical phase), one arrives at the following system of equations:

$$\frac{\mathrm{d}\varepsilon}{\mathrm{d}z'} = -\alpha(1 - e^{-\varepsilon}) - \gamma\varepsilon, \quad (3)$$

$$\frac{\mathrm{d}\varphi}{\mathrm{d}z'} = \frac{1}{2}\frac{\alpha\delta}{\eta}(1 - e^{-\varepsilon}[1 - \eta]), \quad (4)$$

where Eqs. (4) and (5) describe, respectively, the nonlinear transformations in relative pulse energy density (introduced above) and total phase change during the pulse action. The presence of the exponents $e^{-\varepsilon}$stems from the effective two-level scheme of the doping centers: $N_2 = N_0 - N^1$; $N^1 = N_0 e^{-\varepsilon}$; $N^2 = N_0(1 - e^{-\varepsilon})$.

In Eq. (4), the coefficients δ and η concern to the relations between the real and imaginary parts of susceptibilities in the ground (1) and excited (2) states at the chosen wavelength λ, lying within the GSA-transition contour (which is meant to be homogeneously-broaden). These two parameters are defined as follows:

$$\delta = \frac{\chi'^1}{\chi''^1}, \quad (5a)$$

$$\eta = \frac{\chi'^1}{\chi'^2}. \quad (5b)$$

The derived system (3 and 4) addresses the problem of propagation of a resonant pulse through a saturable medium with a single (absorption) resonance, where the first equation (Eq. (3)) is exactly Avizonis-Grotbeck's equation (see Eq. (1)) and shows the interaction of the laser field with the medium and allows one to calculate the nonlinear change of the sample transmission; whilst the second one (Eq. (4)) characterizes the correspondent phase transformation and allows one to calculate the nonlinear change of refractive index, relating to the phase change $\Delta\varphi$ as $\Delta n = \frac{\lambda}{2\pi l}\Delta\varphi$ (l is the sample length).

4.2 *Modeling of refractive index nonlinear change in Co^{2+}: ZnSe (the Z-scan technique)*

For completing the model, one needs to accompany the system (3, 4) by the condition of a Gaussian beam at the sample entrance:

$$\varepsilon^0 = \frac{2E_{\mathrm{p}}}{\pi\omega^2 \mathrm{E_s}}\exp\left(-\frac{2r^2}{\omega^2}\right), \quad (6)$$

$$\psi^0 = Z + k\frac{r^2}{2R}, \quad (7)$$

where r is the radial coordinate; $\omega(Z)$ and $R(Z) = Z + z_0^2/Z$are, respectively, the spot-size and radius of curvature of the beam; Z is the position of the sample with respect to the focus ($Z_0 = 0$, $R_0 \equiv R(Z_0 = 0) = \infty$ and $\omega_0 \equiv \omega(Z_0 = 0)$); $k = 2\pi/\lambda$ and $z_0 = \pi\omega_0^2/\lambda$ are, respectively, the wave number and confocal parameter.

Numerical integration of Eqs.(3) and (4) gives the output (behind the sample of the length l,) characteristics of the beam and Co^{2+}: ZnSe crystal. Knowing the output values $\varepsilon^{\mathrm{out}}$ ($z' = l$) and $\varphi^{\mathrm{out}}(z' = \mathrm{l})$, one can calculate the transmission coefficient, $T0(Z)$, and the refractive index change, $\Delta n^{\mathrm{res}}(Z)$, as:

$$T0(Z) = \frac{\int_0^\infty \varepsilon^{\mathrm{out}} r\,\mathrm{d}r}{\int_0^\infty \varepsilon^{0\mathrm{rdr}}}, \quad (8)$$

$$\Delta n^{\mathrm{PP}}(Z) = \frac{\lambda}{2\pi l}\frac{\int_0^\infty \Delta\varphi\varepsilon^0 r\,\mathrm{d}r}{\int_0^\infty \varepsilon^{0\mathrm{rdr}}}, \quad (9)$$

where

$$\Delta\varphi = \varphi^{\mathrm{out}} - \varphi^0. \quad (10)$$

Finally, let us describe the method to calculate the theoretical dependences of the closed-aperture Z-scans $T1(Z)$(the open-aperture Z-scans $T0(Z)$are given by formula (8)). The Kirchhoff integral for the pulse passing the sample has to be taken over an aperture A (which, being a pinhole, transmits only a very small portion of energy):

$$E(Z) = ik\int_0^\infty E^{\mathrm{out}}\frac{2\pi r\,\mathrm{d}r}{(d - Z)}, \quad (11)$$

where

$$E^{\mathrm{out}}(Z) \propto \sqrt{\varepsilon^{\mathrm{out}}}\mathrm{e}^{-\mathrm{i}\left(\frac{kr^2}{2R} + \frac{kr^2}{2(d-Z)} + \Delta\varphi\right)} \quad (12)$$

and d is the distance between the aperture and focal point. Therefore, $T1(Z)$ is written as follows:

$$T1(Z) = \frac{1}{T0(Z)}\frac{E(Z)E^*(Z)}{E(0)E^*(0)}. \quad (13)$$

5 Analysis of the modeling results and discussion

The calculations have been proceeded for all the Co^{2+}: ZnSe samples whose characteristics are listed in Table 1. Other parameters taken in the calculations are as

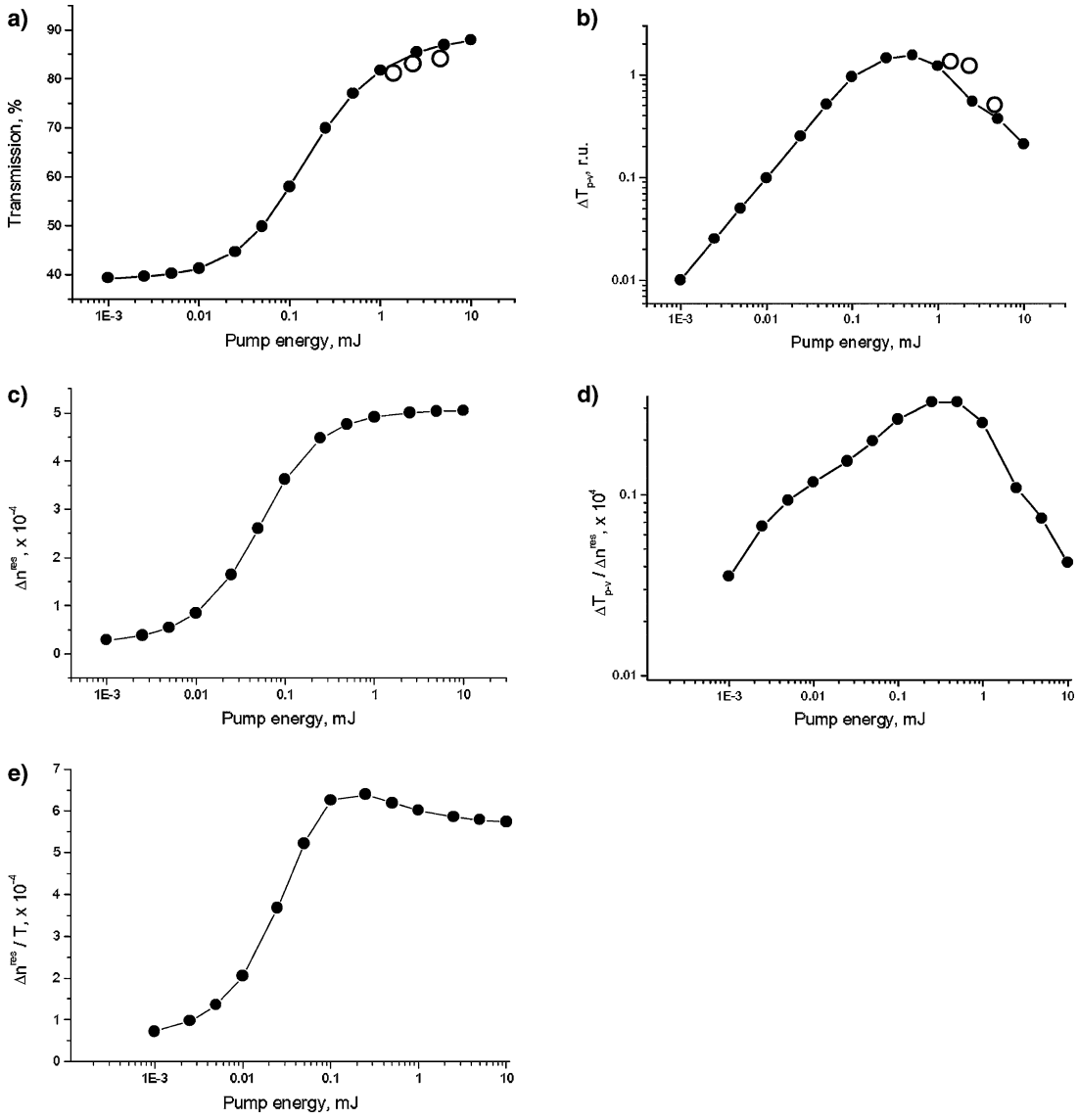

FIGURE 7 Examples of calculated (*lines, filled symbols*) dependences of energy-dependent transmission **a**, magnitude of peak-to-valley oscillation in closed-aperture Z-scans T_{p-v} **b**, nonlinear refractive index change Δn^{res} **c**, and their products VS pulse energy **d, e**. Open symbols in figures **a, b** plot experimental data. All the data were obtained for Co^{2+}:ZnSe sample #355

follows: $E_s = h\nu/\sigma_{GSA} = 0.115$ J/cm^2 [11] (where $\sigma_{GSA} = 11 \times 10^{-19}$ cm^2 and $h\nu = 1.26 \times 10^{-19}$ J for wavelength $\lambda = 1.54$ μm); $\omega_0 = 114$ μm (this value was directly measured in advance to the main experiments); the aperture A coordinate with respect to the beam waist was $Z_1 = 43$ cm. The experimentally measured transmittance of the pinhole (of the diameter $\emptyset = 0.514$ mm) was $\tau = 0.051$; this value, for the chosen setup configuration, is in a perfect agreement with the theoretical estimate: $\tau = 2\emptyset/\pi\omega_1^2 = 0.049$ (where $\omega_1 = \omega(Z_1 = 43\text{ cm}) = 1.85$ mm). The giant pulse energy in calculations was varied within the interval, $E_p = 0$–10 mJ, corresponding to the experimental conditions.

Note that there were no free parameters in the modeling of the energy-dependent transmission of the Co^{2+}: ZnSe samples and the correspondent $T0(Z)Z$-scans (see Eq. (3) and formula (8)), so the theoretical results presented below are as those were obtained with the experimental parameters listed in Table 1. Concerning the equations for the nonlinear change in the phase of a giant pulse passed the Co^{2+}: ZnSe samples and for the correspondent change in refractive index (see Eq. (4) and formulas (9) and (10)) as well as the closed-aperture Z-scans $T1(Z)$ (see formula (13)), we needed to fit only a single free parameter, the ratio η of the real parts of susceptibilities (see formula (5b)), because the value $\delta = 0.205$ for the wavelength $\lambda = 1.54$ μm (see formula (5b)) is directly determined from the experimental absorption spectra (see Fig. 2a) and calculations of the KKR-integral for the real and imaginary parts of susceptibility in the ground state [16]:

$$\chi'^{1}(\Omega) = -\frac{nc}{\pi\Omega} P.V. \int_{-\infty}^{+\infty} \frac{\alpha(\Omega')}{\Omega' - \Omega} d\Omega', \tag{14a}$$

$$\chi''^{1}(\Omega) = \frac{nc\alpha}{\Omega}, \tag{14b}$$

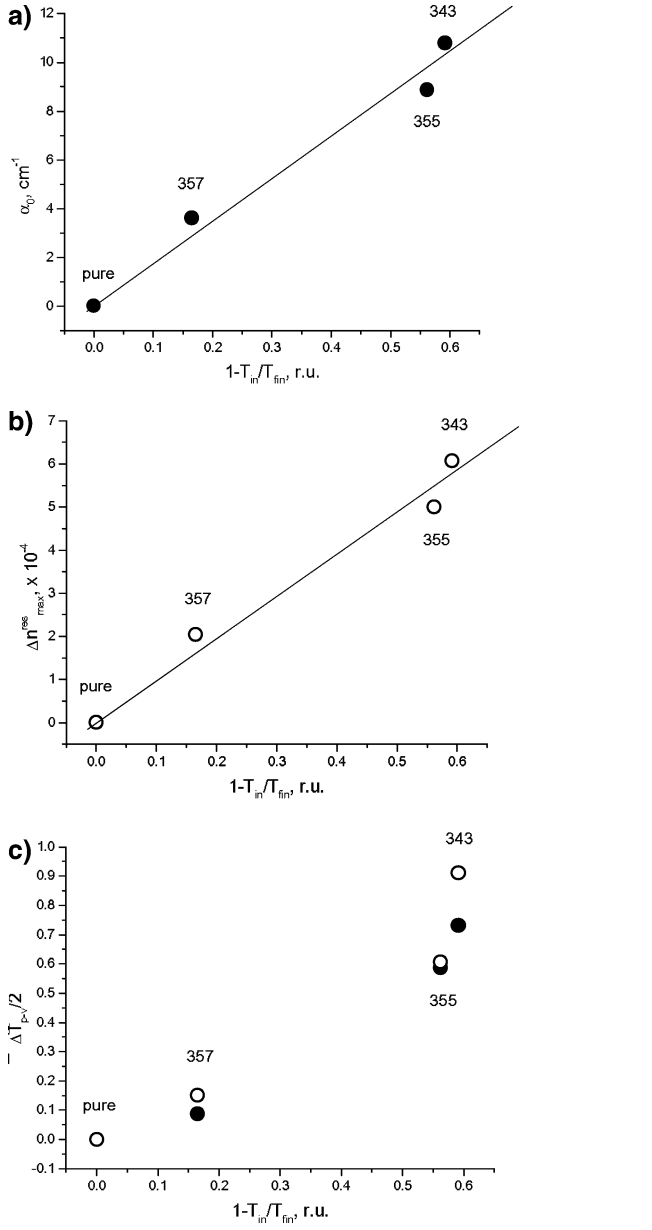

FIGURE 8 Resonant (*weak-signal*) absorption coefficient α **a** (see Table 1), maximal change of refractive index (*in fully-bleached state*) $\Delta n^{\rm res}_{\rm max}$ **b**, and half-magnitude of peak-to-valley oscillation in closed-aperture Z-scans $T_{p-v}/2$ **c** VS parameter $1 - T_{\rm in}/T_{\rm fin}$ for samples #343, #355, and #357 (*labels are given directly on the graphs*). Filled and open symbols relate, respectively, to experimental and theoretical data

(Ω is the angular optical frequency). The results of these calculations are shown in Fig. 2b and c. Finally, fitting by η of all the experimental data gave us the following value of the ratio η: $\eta = 0.043$.

The results of the final modeling are shown in Figs. 4, 5b, 7, and 8. A comparison of Fig. 4a–c and 5b with their experimental counterparts (Figs. 3(a-c) and 5(a)) allows one to conclude on their remarkable agreement, testifying for an appropriate validity of our theory that addresses the nonlinear change in refractive index $\Delta n^{\rm res}$ in Co^{2+}: ZnSe (see Fig. 4d) as well as for modeling the open and closed aperture Z-scans. Fig. 7 shows (by filled circles) an example of the modeling (for the Co^{2+}: ZnSe sample #355) of the energy-dependent transmission (a), nonlinear refractive index change (c), the correspondent magnitude of the peak-to-valley oscillation in the closed-aperture Z-scans $T\,1(Z)$ (b), and also their products (d, e). On the plots (a, b) are also shown (by open circles) the experimental data taken from Fig. 5a). One can notice that our experiment was performed for a "deep" saturating of the crystals' absorption (where $\varepsilon \gg 1$). Note that signals registered experimentally (with the aperture A of the transmittance $\tau \approx 5\%$, see above) allowed us to work with an appropriate accuracy of the measurements at pulse energies exceeding at least 0.5 mJ. On the other hand, this arrangement allowed getting maximal values of the resonant refractive index change in Co^{2+}: ZnSe. As is seen from Fig. 4d), this quantity is about of units of 10^{-4} at the chosen wavelength and can be determined from the modeling only, since at the deep saturating the correspondent $T\,1(Z)$and$T0(Z)$ Z-scans are seriously deforming and a simple measurement of the peak-to valley transmission ΔT_{p-v} (nearly the $Z_0 = 0$ point) as an indicator of the maximal values of $\Delta n^{\rm res}$ is impossible. Figure 8 demonstrates some important (experimental and theoretical) parameters of the tested Co^{2+}: ZnSe samples – the resonant (weak-signal) absorption (a), the maximal change of refractive index (in fully-bleached state) (b), and the magnitude of the peak-to-valley oscillation in the closed-aperture Z-scans $T\,1(Z)$(c) – as the dependences of the $1 - T_{\rm in}/T_{\rm fin}$ parameter. A comparison of the dependences (b) and (c) in Fig. 8 testifies for the above conclusion that, despite the oscillation ΔT_{p-v} (c) predicts qualitatively the behavior of the change $\Delta n^{\rm res}_{\rm max}$ (b), the latter may be quantitatively found from the modeling only.

6 Conclusions

We have performed an experimental study of the energy-dependent transmission coefficient and nonlinear change $\Delta n^{\rm res}$ in refractive index in a set of Co^{2+}: ZnSe samples prepared applying the novel technology (diffusion at the equilibrium condition, S_{ZnSe}-S_{CoSe}-L_{Zn}-V). Experimentally, these characteristics have been obtained by measuring the open-aperture ($T\,0(Z)$) and closed-aperture ($T\,1(Z)$) scans with the use of the well-known Z-scan single-beam technique adapted for the case of the resonant non-linearity at the wavelength 1.54 μm and short-pulse probing. The experiments have been conducted with Co^{2+}:ZnSe samples, having different concentrations of Co^{2+} ions, at different GSA saturation levels (i.e., at different energies E_p of the probe pulse, but fixed focusing arrangement). The experimental results obtained have been modeled applying (i) a novel system of equations (3 and 4), allowing one to calculate the resonant nonlinear refraction in a doped saturable material at the short-pulse excitation, and (ii) an adequate model for the Z-scan technique adapted to these circumstances. We have demonstrated that the nonlinear change in refractive index in Co^{2+}: ZnSe strongly depends on pulse energy and that its maximal attainable value is about 10^{-4} at the wavelength $\lambda = 1.54$ μm. Notice that the experimental and theoretical results presented above are in a reliable agreement and allows one to apply the developed approach for studying the resonant non-linearities in other doped materials.

ACKNOWLEDGEMENTS This work has been partially supported by the Russian Fund for Basic Research #03-02-17316 (Russian Federation). A.V. Kir'yanov ackowledges financial support from the Consejo Nacional de Ciencia y Tecnologia (CONACyT, Mexico) for his sabbatical period.

REFERENCES

1 M. Birnbaum, M.B. Camargo, S. Lee, F. Unlu, R.D. Stultz, OSA TOPS—Advanced Solid State Lasers, **10** 148 (1997)
2 A.V. Podlipensky, V.G. Shcherbitsky, V.P. Mikhailov, N.V. Kuleshov, OSA TOPS—Advanced Solid State Lasers, **34**, 249 (2000)
3 V.N. Filippov, A.N. Starodumov, A.V. Kir'yanov, Opt. Lett. **26**, 343 (2001)
4 A.V. Kir'yanov, V.N. Filippov, A.N. Starodumov, J. Opt. Soc. Am. B **19**, 353 (2002)
5 L.D. DeLoach, R.H. Page, G.D. Wilke, S.A. Payne, W.F. Krupke, IEEE J. Quant. Electron. **32**, 885 (1996)
6 S.B. Mirov, V.V. Fedorov, K. Graham, I.S. Moskalev, V.V. Badikov, V. Panyutin, Opt. Lett. **27**, 909 (2002)
7 A.V. Podlipensky, V.G. Shcherbitsky, N.V. Kuleshov, V.P. Mikhailov, V.I. Levchenko, V.N. Yakimovich, Opt. Lett. **24**, 960 (1999)
8 Z. Burshtein, Y. Shimony, R. Feldman, V. Krupkin, A. Glushko, E. Galun, Opt. Mater. **15**, 285 (2001)
9 T.W. Tsai, M. Birnbaum, J. Appl. Phys. **87**, 25 (2000)
10 V.G. Shcherbitsky, S. Girard, M. Fromager, R. Moncorge, N.V. Kuleshov, V.I. Levchenko, V.N. Yakimovich, B. Ferrand, Appl. Phys. B **74**, 367 (2002)
11 N.N. Il'ichev, P.V. Shapkin, S.E. Mosaleva, A.S. Nasibov, Quant. Electron. **34**, 1169 (2004)
12 N.N. Il'ichev, A.V. Kir'yanov, P.P. Pashinin, S.M. Shpuga, Sov. Phys. JETP, **78**, 768 (1994)
13 A. Brignon, J. Opt. Soc. Am. B **13**, 2154 (1996)
14 P.V. Avizonis, R.L. Grotbeck, J. Appl. Phys. **37**, 687 (1966)
15 R.A. Betts, T. Tjugiarto, X.L. Xue, P.L. Chu, IEEE J. Quant. Electron. **27**, 908 (1991)
16 D.C. Hutchings, M. Sheik-Bahae, D.J. Hagan, E.W. VanStryland, Opt. Quant. Electron. **24**, 1 (1992)
17 I.T. Sorokina, Optical Materials **26**, 395 (2004)
18 A.V. Kir'yanov, Y.O. Barmenkov, Appl. Phys. B **77**, 613 (2003)
19 M. Sheik-Bahae, A.A. Said, T.H. Wei, D. Hagan, E.W. VanStryland, IEEE J. Quant. Electron. **26**, 760 (1990)
20 M. Sheik-Bahae, A.A. Said, E.W. VanStryland, Opt. Lett. **14**, 995 (1989)
21 V.I. Levchenko, V.N. Yakimovich, L.I. Postnova, V.I. Konstantinov, V.P. Mikhailov, N.V. Kuleshov, J. Cryst. Growth **198/199**, 980 (1999)
22 Z. Mierczyk, A. Majchrowski, I.V. Kityk, W. Gruhn, Opt. Laser Technol. **35**, 169 (2003)
23 M. delRayo, Yu.O. Barmenkov, A.V. Kir'yanov, A.N. Starodumov, J. Vanhanen, T. Jaaskelainen, Laser Phys. **11**, 502 (2001)